JOURNAL OF CATALYSIS 99, 449–460 (1986)

The Effect of Reduction Conditions on the Chloride Content of Ir/TiO_2 Catalysts and Their Activity for Benzene Hydrogenation

LE VAN TIEP,* MONIQUE BUREAU-TARDY,* GUY BUGLI,*
GERALD DJEGA-MARIADASSOU,* MICHEL CHE,† AND GEOFFREY C. BOND‡

*Laboratoire de Cinétique Chimique, Université P. and M. Curie, 1 Rue Guy de la Brosse, 75005 Paris, France; †Laboratoire de Réactivité de Surface et Structure, U.A. 1106, CNRS, 4 Place Jussieu, 75230 Paris, France; and ‡Department of Chemistry, Brunel University, Uxbridge UB8 3PH, United Kingdom

Received August 23, 1985; revised January 10, 1986

Reduction of K_3IrCl_6 on TiO_2 occurs in two well-defined stages, the first of which occurs between 350 and 470 K and consumes an amount of H_2 independent of Ir content. No HCl is released during this stage. It is suggested that $IrCl_6^{3-}$ ions interact with Ti—OH groups to form a monolayer of $IrCl_x(O—Ti)_{6-x}$ species which on reduction afford highly dispersed Ir particles (1–2.5 nm), and that HCl formed by elimination and during reduction chlorinates other Ti—OH groups. K_3IrCl_6 in excess of that required to form a monolayer exists as less reducible microcrystals leading to larger Ir particles on reduction. Complete removal of Cl^- under H_2 cannot be achieved. The effect of precalcination, and of oxidation after reduction, on the Cl^- content has been examined. Residual Cl^- affects the O_2 titration of chemisorbed H, giving anomalously low results for the number of surface Ir atoms. Resulting turnover frequencies (TOF) are therefore unreliable, but Ir/TiO_2 reduced at low temperature shows specific activity for benzene hydrogenation comparable to that for Ir/SiO_2. Low TOF's for Ir/TiO_2 after high-temperature reduction are attributed to crowding of free sites by TiO_{2-x} species. The role of Cl^- in TiO_2-supported catalysts needs a complete reappraisal.

INTRODUCTION

We have already examined the evolution of HCl during the reduction of $RhCl_3/Al_2O_3$ catalysts, and the effect of residual Cl^- on the activity for benzene hydrogenation (*1*). Interactions between the support and chlorinated precursors of the metal were shown to affect initial and final temperatures of reduction and of dechlorination, but in agreement with previous work by Basset *et al.* (*2*) no effect of Cl^- on the catalytic activity was observed. In contrast, Vannice and Chou (*3*) have recently shown that a correlation may exist between addition of HCl to a reduced Pd/TiO_2 catalyst and subsequent increases in dispersion and in activity for this reaction. Rate increases of 5 to 10 times were observed at low reduction temperature (448 K), so this enhancement was not connected with a strong metal–support interaction (SMSI).

A more complex situation may exist with TiO_2-supported metals formed from chloride salts, where the SMSI phenomenon may be superimposed on the effects of Cl^-. The SMSI effect, now usually attributed to the migration of reduced fragments of the support (TiO_{2-x}) onto the metal particles (*4, 5*), produces a marked decrease in capacity for chemisorbing both H_2 and O_2, as well as in activity for structure-sensitive reactions such as alkane hydrogenolysis (*6*). Chemisorption capacity is restored by oxidation followed by low-temperature (473 K) reduction (*7*); the activity decrease is not due to sintering.

In preparing supported Pt catalysts, calcination is sometimes carried out either before or after reduction (*8–10*), and a detailed study has been made (*9*) of the reduction of the various complexes which are thought to be formed. The use of temperature-programmed reduction (TPR) in conjunction with measurement of HCl evolution should assist our understanding of re-

0021-9517/86 $3.00

duction steps and their correlation with catalytic activity.

Two kinds of result can therefore be expected in the reduction of TiO_2-supported chloride salts: (i) after low-temperature (473 K) reduction (LTR), a possible enhancement in the specific activity for benzene hydrogenation, which is well-known to be a structure-insensitive reaction; and (ii) after high-temperature (773 K) reduction (HTR), a decrease in activity due to the SMSI. In this paper we investigate the mode of reduction of K_3IrCl_6/TiO_2 to give Ir/TiO_2 catalysts having a known Cl^- content. TPR and HCl evolution measurements have been made in parallel in order to define and compare reduction and dechlorination steps, and to elucidate the structure of intermediate species in the formation of the catalyst. Benzene hydrogenation has been used as the test reaction to follow the dependence of catalytic activity on pretreatment conditions.

EXPERIMENTAL

Precursors to Ir/TiO_2 catalysts were prepared by impregnating Degussa P-25 TiO_2 (20% rutile, 80% anatase, 50 $m^2\ g^{-1}$) with an aqueous solution of $K_3IrCl_6 \cdot H_2O$ (Johnson Matthey Chemicals plc): metal loadings were 0.8, 1.6, and 3.2 wt% after reduction. The preparations are designated I 0.8(Cl), I 1.6(Cl), and I 3.2(Cl), respectively. Ir/SiO_2 was made by the same technique using Degussa Aerosil and an acidic solution of H_2IrCl_6. Ir/TiO_2 (2 wt%) was prepared from a Cl^--free precursor, $[Ir(NH_3)_5H_2O](NO_3)_3$, deposited on P-25 TiO_2 preexchanged with an ammonia solution: this is designated E 2 (NH_3). KCl/TiO_2 (2.9 wt%) was also prepared by impregnation.

Catalysts were characterized by H_2—O_2 titration performed gravimetrically at room temperature using a Setaram microbalance type MTB 10-8, sensitivity 10^{-5} g (*11*). The main steps were taken to be, as in the case of Ir/Al_2O_3 (*12*),

$$Ir_s\text{—}H + \tfrac{3}{4}O_2 = Ir_s\text{—}O + \tfrac{1}{2}H_2O_{ads} \quad (1)$$

$$Ir_s\text{—}O + \tfrac{3}{2}H_2 = Ir_s\text{—}H + H_2O_{ads} \quad (2)$$

With Ir/TiO_2 catalysts, water produced in step 2 apparently remains adsorbed on the catalyst since no decrease in weight was observed. Selected catalysts were examined by high-resolution transmission electron microscopy using a JEM 100 CX II THG 1 instrument. TPR measurements were made in a conventional system using katharometer detection, 6% H_2 in N_2 at 40 $cm^3\ min^{-1}$ and a heating rate of 5 K min^{-1} from ambient to 873 K. Three kinds of experiment were performed: (i) TPR after a precalcination of the adsorbed salt at 623 K for 1.5 h in air (TPR-Ox); (ii) TPR of the adsorbed salt without prior treatment after drying (TPR-I); and (iii) TPR-II after TPR-I and subsequent calcination in air at 623 K for 1.5 h. HCl evolution measurements were made conductimetrically as previously described (*1*). Rates of benzene hydrogenation were measured at atmospheric pressure in a conventional dynamic differential reactor (*1*). Thermogravimetric (TGA) and differential thermal analysis (DTA) were carried out in either a Setaram Type BGO thermobalance or in a Stanton Redcroft STA-780 apparatus.

RESULTS

TGA/DTA and TPR of Precursors

Study of the reduction of unsupported $K_3IrCl_6 \cdot H_2O$ by TGA/DTA showed that dehydration occurred at about 376 K: reduction started at 413 K and was complete according to Eq. (3) at 563 K.

$$K_3IrCl_6 + \tfrac{3}{2}H_2 = Ir^0 + 3HCl + 3KCl \quad (3)$$

KCl supported on TiO_2 when heated under H_2 evolved HCl at about 673 K. The decomposition in air of the precursor to catalyst E 2(NH_3) began with a 1.6% weight loss between ambient and 473 K (adsorbed water), but the principal weight loss occurred in a complex exothermic process between 473 and 623 K: the product was presumably an iridium oxide.

Figure 1 shows the TPR results for the

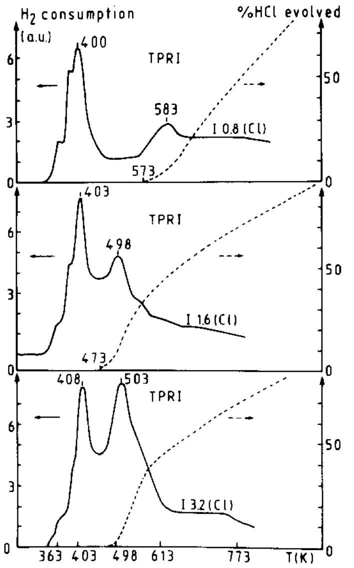

FIG. 1. Results of TPR-I experiments for three different Ir contents (0.8, 1.6, and 3.2 wt%). Total flow rate, 46 cm^3 min^{-1}; 6% H_2 in N_2; heating rate, 5 K min^{-1}.

three precursors containing the chloride salt (TPR-I); Fig. 2 compares TPR-I, TPR-II, and TPR-Ox for the material containing 1.6 wt% Ir. In each case the reactions proceed in two quite clearly defined stages, the minimum between them occurring at about 473 K. In TPR-I experiments, the first stage of the reduction of the chloride occurs in three poorly resolved steps having T_{max} values of, respectively, 363, 378 ± 5, and 405 ± 3 K (Fig. 1). The size of the first two steps diminishes with respect to the third as the Ir content increases, but approximate manual deconvolution of the two main stages suggests that the H_2 consumption for the first stage is about constant (~43 mol μg_{cat}^{-1}, Table 1): the H/Ir_{tot} ratio therefore decreases with increasing Ir content. The contribution of the second stage increases as the Ir content is raised (Fig. 1 and Table 2), but the H/Ir_{tot} ratio summed over both stages decreases with increasing Ir content (Table 3).

Oxidation after TPR-I (i.e., TPR-II) gives materials which still reduce in two stages (Fig. 2 and Tables 1 and 2): values of T_{max} are, respectively, 363 ± 10 and 480 ± 10 K, but the H_2 consumption in the first stage, still reasonably constant for a given metal loading, now increases with Ir content (Table 1) while the combined H/Ir_{tot} ratio (Table 3) is somewhat lower than the value of three which is expected if the oxidation after TPR-I leads to the formation of Ir_2O_3. Reduction of precalcined samples (TPR-Ox) also occurs in two stages (Fig. 2 and Tables 1–3), and the H/Ir_{tot} ratios summed

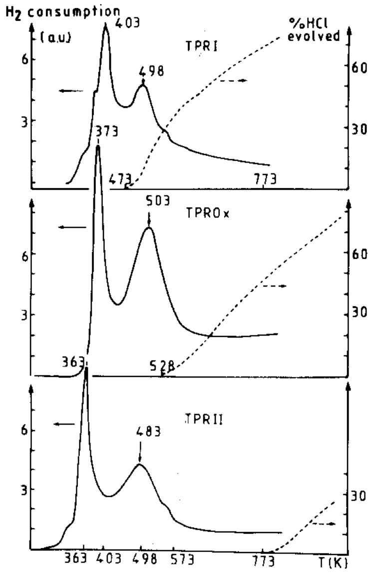

FIG. 2. Results of TPR experiments for I 1.6 (Cl) (TPR-I, TPR-Ox, and TPR-II). Conditions as in Fig. 1.

TABLE 1

TPR Results for the First Peaks

Catalyst	TPR-Ox	TPR-I	TPR-II
	15.6[a]	44.2	13.8
I 0.8(Cl)	0.75[b]	2.1	0.7
	402[c]	400	373
	45.1	43.7	37.5
I 1.6(Cl)	1.1	1.05	0.9
	373	403	363
	38.8	4.15	52.2
I 3.2(Cl)	0.5	0.5	0.6
	408	408	353

[a] V (μmol g_{cat}^{1}).
[b] H/Ir.
[c] T_M (K).

TABLE 2

TPR Results for the Second Peaks

Catalyst	TPR-Ox	TPR-I	TPR-II
I 0.8(Cl)	7.6[a]	8.7	6.7
	0.35[b]	0.40	0.30
	503[c]	583	488
I 1.6(Cl)	63.4	43.3	42.4
	1.5	1.05	1.0
	503	498	483
I 3.2(Cl)	74.1	72.3	41.5
	0.9	0.85	0.5
	518	503	473

[a] V (μmol g_{cat}^{-1}).
[b] H/Ir.
[c] T_M (K).

over both stages are again somewhat low (Table 3).

Reduction of the supported ammine complex also occurs in two unequal stages (Fig. 3 and Table 4) but the T_{max} values are much higher than those for the chloride salt and its oxidized derivatives. The stoichiometric equation for reduction of the ammine complex may be written as

$$[Ir(NH_3)_5H_2O](NO_3)_3 + \tfrac{27}{2}H_2 = Ir^0 + 8NH_3 + 10H_2O \quad (4)$$

for which the H/Ir ratio would be 27: the observed value of 28.8 is in good agreement. Calcination before reduction leads to a single major peak for which T_{max} = 358 K and H/Ir = 2.4 (Fig. 3): the product of the oxidation is thus probably supported Ir_2O_3.

HCl Evolution

Figure 1 also demonstrates the manner of evolution of HCl measured conductimetrically as samples were heated in pure H_2. For untreated samples (corresponding to TPR-I) HCl evolution only starts above 473 K: HCl produced during the first reduction stage must therefore remain adsorbed. Its evolution corresponds to the second stage of H_2 consumption but continues beyond it: it starts a little below the temperature at which desorption of HCl preadsorbed onto TiO_2 begins. Reduction after subsequent oxidation (i.e., TPR-II) shows that no HCl is evolved below 773 K (Fig. 2). Reduction of the precalcined precursor (i.e., TPR-Ox) shows no HCl evolution related to the first H_2 consumption stage, although it appears simultaneously with the second

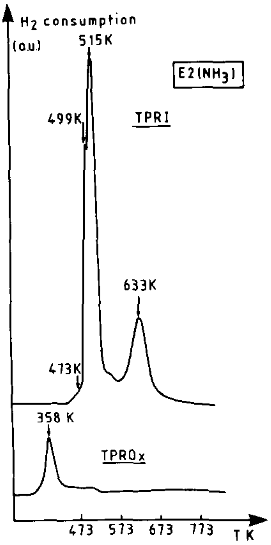

FIG. 3. TPR of E 2(NH_3). Conditions as in Fig. 1.

TABLE 3

ΣH/Ir Ratios According to the Type of TPR Experiment

Catalyst	TPR-Ox	TPR-I	TPR-II
I 0.8(Cl)	1.1	2.5	1.0
I 1.6(Cl)	2.6	2.1	1.9
I 3.2(Cl)	1.4	1.35	1.1

TABLE 4

TPR-I for a 2 wt% Ir/TiO_2 Catalyst (Precursor: $[Ir(NH_3)_5H_2O](NO_3)_3$)

T_M (K)	H_2 uptake (mmol g_{cat}^{-1})	H/Ir
515	1.06	20.4
633	0.44	8.4
Total	1.50	28.8

TABLE 5

Chloride Evolution during TPR Experiments for I 1.6(Cl) Catalyst According to Pretreatment

Expt	Pretreatment	Weight of sample (mg)	Initial dechlorination temperature (K)	Final experimental temperature (K)	$HCl \times 10^6$ evolved (mol)		Residual Cl^- (experimental)
					Theoretical	Experimental	
1	N_2, 298, (1); experiment conducted in flowing N_2 (thermal decomposition)	202.7	623	1123	101	79.3	21.7
2	N_2, 298, (1) H_2, 298, (0.5) TPR-I	502	573	473[a]	252.6	19.6	233
3	N_2, 298, (0.5) H_2, 298, (0.5) TPR-I	201.3	473	823	101	61	40
4	N_2, 298, (0.7) H_2, 298, (0.5) TPR-I	200	476	1123	101	90	11
5	O_2, 623, (1.5) N_2, 298, (19) H_2, 298, (0.5) TPR-Ox	198	528	1123	—	60	—
6	R823 (Expt 3) O_2, 623, (1.5) N_2, 298, (1), H_2 298, (0.5) TPR-II	195.4	773	1123	—	20.7	—

Note. N_2, 298, (0.7) represents flowing nitrogen at room temperature during 0.7 h. TPR-Ox, TPR-I, and TPR-II symbolize the type of TPR according to the pretreatment.

[a] The heating was stopped at exactly 473 K but due to furnace inertia the temperature of the sample rose slightly above 473 K before decreasing, leading to approximately 8% HCl evolved.

stage. The same H_2 consumption is observed as in the case of the TPR-I experiment.

Table 5 shows some quantitative results of HCl evolution measurements made with catalyst I 1.6(Cl). Thermal decomposition under N_2 to 1123 K (Expt 1) afforded only 80% of the theoretical amount of Cl^-, and HCl evolution only started at 623 K. Heating under H_2 to 473 K gave only 8% of the total Cl^- present as HCl (Expt 2), notwithstanding the fact that about half the total H_2 uptake took place below this temperature in TPR-I (Fig. 1, Tables 1 and 2). Increasing the final temperature to 823 and 1123 K (Expts 3 and 4) led, respectively, to the recovery of 61 and 90% of the total Cl^-. Reduction of the chloride salt according to the equation

$$K_3IrCl_6 + \tfrac{3}{2}H_2 = Ir^0 + 3HCl + 3KCl \quad (5)$$

would suggest that at most one-half of the Cl^- should be released: the observed values suggest that KCl can decompose with the evolution of further HCl. Residual K^+ may not be without effect on the capacity of the catalysts to form and to dispose of carbonaceous overlayers.

Reduction after prior calcination showed (Expt 5) the appearance of HCl above 528 K, the total amount formed being about 60% of that originally present. Some HCl was formed in the analog to TPR-II above 773 K (Expt 6); neither the first reduction nor the subsequent oxidation succeeded in achieving complete dechlorination.

Oxygen Titration and Catalytic Activity

Table 6 reports the principal results obtained by O_2 titration (OT) of preadsorbed H and by measuring the rate of benzene hydrogenation. The number of sites estimated by OT is about the same after reduction at 449 and 823 K, but the dispersions to which these values correspond are much lower, and the derived particle sizes much higher, than those revealed by electron microscopy. This technique does however confirm the absence of sintering on high-temperature reduction, but it also reveals the presence of a few large (~10 nm) particles (see Fig. 4) which would serve to decrease the average dispersion slightly.

A number of the Arrhenius plots for benzene hydrogenation are shown in Fig. 5 and some of the derived activation energies are contained in Table 6. For samples reduced at low temperature (LTR), values are independent of Ir content (32–38 kJ mol^{-1}), but there is a greater range for catalysts reduced at high temperature (HTR) (27–53 kJ mol^{-1}). Ir/SiO_2 shows a value of 42 kJ mol^{-1}. These values are to be compared with that of 35.6 kJ mol^{-1} for Rh/Al_2O_3 (*1*, *13*), which is similar to those reported for Pt/Al_2O_3 (*2*), Pt/SiO_2, and Ru/SiO_2 (*14*). Supported Pd catalysts show values between 33 and 46 kJ mol^{-1} (*3*).

TABLE 6

Number of Sites and Activity of Ir/TiO_2 Catalysts in Benzene Hydrogenation ($P^0_{C_6H_6}$ = 60 mm Hg; $P^0_{H_2}$ = 700 mm Hg at 339 K)

	Apparent number of sites (g_{Ir}^{-1})	Apparent metallic surface area ($m^2\ g_{Ir}^{-1}$)	Apparent percentage exposed, *D*	Particle size (nm)	Specific rate at 339 K (mol s^{-1} g_{Ir}^{-1})	Activation energy (kJ mol^{-1})	Apparent TOF at 339 K (s^{-1})
I 0.8(Cl)R480	—	—	—	—	5.1×10^{-3}	37.6	—
I 0.8(Cl)R833	—	—	—	—	9.1×10^{-6}	26.7	—
I 1.6(Cl)R449	2.8×10^{20} 11.17[a]	24.3	9	10[c] 0.9 to 2.5[d]	1.4×10^{-3}	36.4	3
I 1.6(Cl)R473[b]	—	—	—	—	1.4×10^{-3}	—	—
I 1.6(Cl)R823	2.35×10^{20} 9.37[a]	20.4	7.5	12[c] 0.9 to 2.5[d]	2.8×10^{-5}	53.1	0.07
I 3.2(Cl)R453	—	—		—	2.3×10^{-4}	31.8	—
I 3.2(Cl)R793	2.0×10^{20} 7.97[a]	17.4	6.4	14.1[c] —	16.7×10^{-6}	38.4	0.05
E 2(NH_3)R523	—	—	—	—	1.15×10^{-3}	—	—
E 2(NH_3)R833	—	—	—	—	3.6×10^{-4}	—	—
1% Ir/SiO_2	5.4×10^{20} 21.5[a]	47	17	5[c] 2.5[d]	2.3×10^{-4}	41.8	0.25

[a] Raw oxygen uptakes in H_2–O_2 titrations (mg O_2 g_{Ir}^{-1}).

[b] Sample quenched at 473 K.

[c] $d = 90/D$.

[d] Electron microscopy.

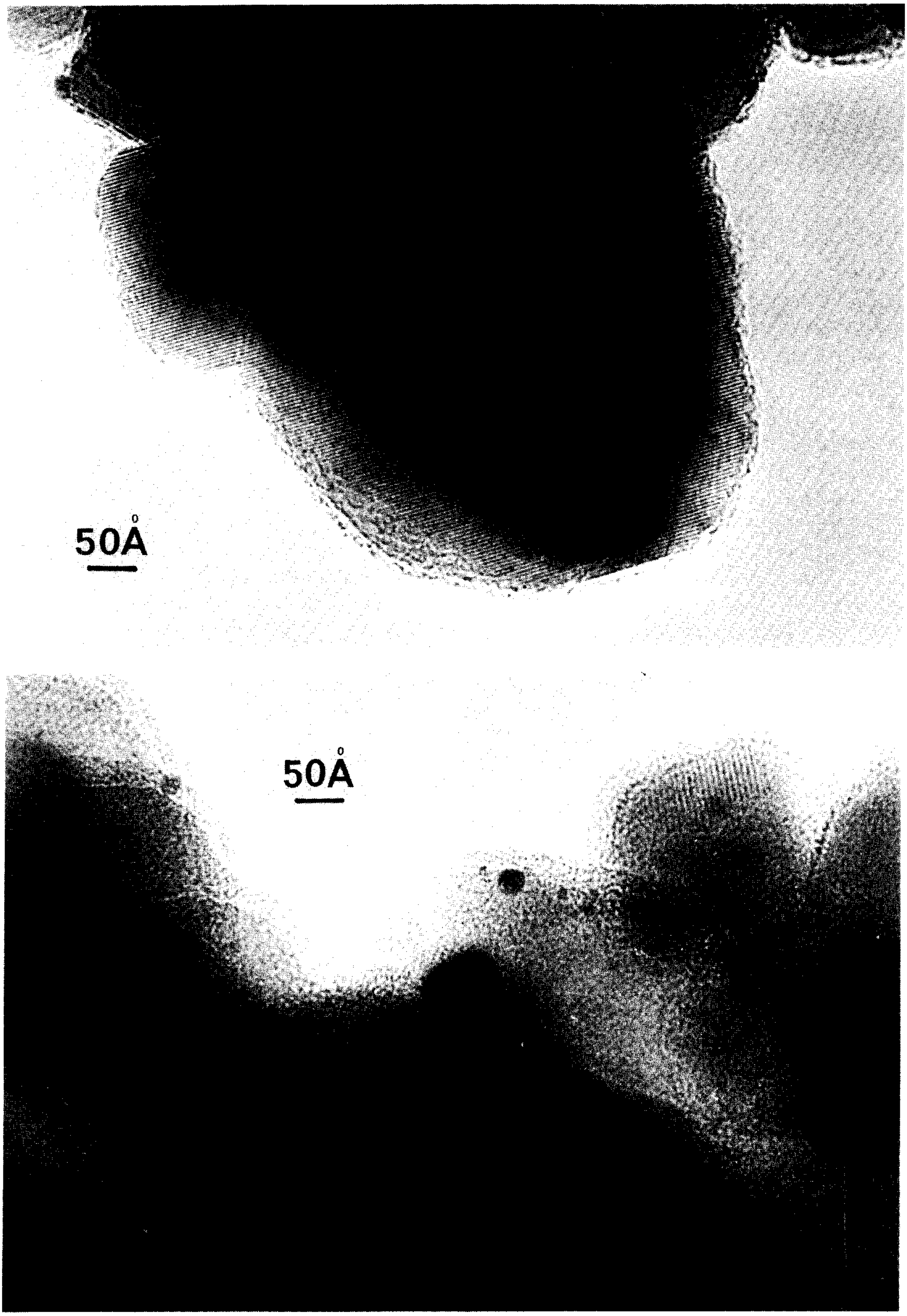

FIG. 4. Transmission electron micrographs for I 1.6 (Cl).

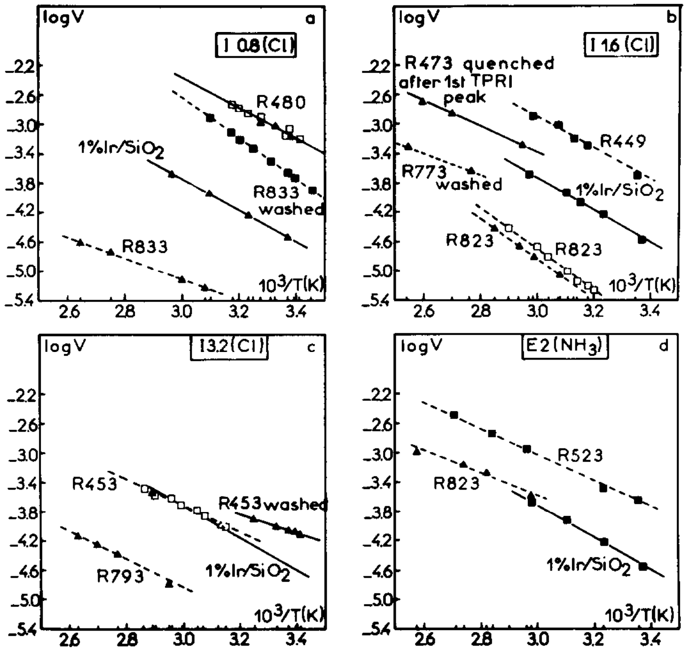

FIG. 5. Arrhenius plots for benzene hydrogenation after various reductions and pretreatments.

Table 6 also gives specific rates (mol g_{Ir}^{-1} s^{-1}). The 1% Ir/SiO_2 may be taken as the reference point, since its dispersion is probably similar to that of the TiO_2 supported catalysts (Table 6): its specific rate is not a function of reduction temperature (*15*). What is most noticeable in Fig. 4 is that all the LTR catalysts are *more* active than the Ir/SiO_2. Table 7 shows the ratio of the observed rates at 339 K for each LTR Ir/TiO_2 catalyst to that for Ir/SiO_2: the value increases with diminishing Ir content. The HTR catalysts derived from the chloride salt are however all *less* active than Ir/SiO_2. That derived from the ammine complex (i.e., E 2(NH_3)) is not apparently deactivated by HTR. Washing with water after HTR leads to a partial restoration of activity (Figs. 5a,b). However, washing after LTR (Fig. 5c) also gives higher activity, but this can have no connection with SMSI. In each case Cl^- was detected in the filtrate.

Figure 5b shows that the activity produced by reduction to 473 K (i.e., just past the first stage in the TPR) is only marginally less than that given by 3 h reduction at 449 K. This suggests that the majority of the active sites are produced in the first stage of the reduction, and that the second stage produces relatively few.

Finally we have estimated turnover frequencies (TOF) on the basis of the OT results (Table 6). The value for Ir/SiO_2 (0.25 s^{-1}) agrees well for that found for Rh/Al_2O_3 at the same temperature (1 s^{-1}) (*1, 13*), but is higher than those quoted for supported Pd catalysts at 413 K (0.060 ± 0.025 s^{-1}) (*3*). On the assumptions that benzene hy-

TABLE 7

Ratio of the Specific Rates (mol s^{-1} g_{Ir}^{-1}) in Benzene Hydrogenation Relative to 1 wt% Ir/SiO_2, Calculated at 339 K

Catalyst	Low T_R[a]	Ratio[b]	High T_R[a]	Ratio[b]
I 0.8(Cl)	480	22	833	0.04
I 1.6(Cl)	473	6	823	0.1
I 3.2(Cl)	453	1	793	0.07
E 2(NH_3)	523	5	823	1.6

[a] T_R = reduction temperature (K).

[b] Ratio = ($V_{catalyst}/V_{Ir/SiO_2}$).

drogenation is a truly structure-insensitive reaction and that there is no metal–support interaction to affect Ir/TiO_2 relative to Ir/SiO_2, one would expect TOF's to be the same for each support and to be independent of reduction temperature. However, the value for I 1.6(Cl) after LTR is much higher and after HTR considerably lower than that for Ir/SiO_2.

DISCUSSION

The results presented above show a number of unusual and surprising features. They indicate the importance of careful and detailed study of the processes whereby the precursor is transformed into the active catalyst, and of the choice of the metal salt employed. The first observations requiring discussion are those concerning the TPR and HCl evolution during reduction of supported K_3IrCl_6. Figure 1 showed that this salt was reduced in two stages, the first of which consumed an amount of H_2 almost independent of Ir content but which was subdivided into three steps: little or no HCl was evolved during this first stage. We have also shown with catalyst I 1.6(Cl) that this stage generates catalytically active Ir^0 (Fig. 5). We therefore suggest that HCl formed at this time immediately attacks the TiO_2 surface, replacing OH^- groups by Cl^- (*16*):

$$\text{Ti—OH} + \text{HCl} = \text{Ti—Cl} + H_2O \quad (6)$$

HCl evolution only begins to be significant above about 473 K, which corresponds approximately to the start of the second stage of H_2 uptake, although the two events are not necessarily causally connected. Some of the Cl^- is retained to very high temperature (Table 5). It is possible that HCl is evolved by reversal of Eq. (6) if water remains bonded to the surface, but to establish the exact mechanism of release of Cl^- under reducing conditions will require further work. Certainly HCl is formed at high temperature without the use of H_2. Similar observations have recently been made with $RuCl_3/TiO_2$ (*17*) and are reminiscent of those seen in the reduction of $PdCl_2/SnO_2$ (*18*).

The TPR and HCl evolution measurements allow us to develop a reasonably detailed picture of the structure of the precursor after drying and of the processes occurring during activation. We suppose that during drying there is formed a monolayer of Ir complexes by reaction of $IrCl_6^{3-}$ with Ti—OH groups:

$$IrCl_6^{3-} + x(\text{Ti—OH}) = IrCl_{6-x}(\text{O—Ti})_x + x\text{HCl} \quad (7)$$

where x probably takes values between 1 and 3. The validity of this hypothesis can be checked in four ways (see Appendix). (i) If the reduction of the adsorbed chloro-complexes constitutes the first stage of the total process, the amount of H_2 used (~43 μmol g_{cat}^{-1}, Table 1) based on reduction of Ir^{III} to Ir^0 is equivalent to 1.7×10^{19} molecules of $IrCl_6^{3-}$. (ii) If $IrCl_6^{3-}$ ions were to form a close-packed array, each occupying an area of 0.67 nm^2, the number which could be accommodated is 7.4×10^{19} per g. (iii) If there are 4.5 OH groups nm^{-2} (*19*), the minimum number of adsorbed complexes which could be formed, corresponding to $x = 3$ in Eq. (7), is 3.7×10^{19} per g assuming that each HCl molecule formed chlorinates one further OH group. (iv) We note that the Ir loading of 0.8 wt%, where TPR-I shows most of the H_2 to be consumed in the first stage, corresponds to 2.5×10^{19} molecules of $IrCl_6^{3-}$ per g. There are of course many assumptions made in these rough calculations, but the similarity of the numbers obtained suggests that the great majority of OH groups react with a part of the Ir salt by Eq. (7) to give a highly dispersed and partially dechlorinated precursor state; this forms a virtual monolayer over the TiO_2 surface, and involves most of the Ti—OH groups. The number of Ir atoms in this monolayer is $2.7 \pm 1.0 \times 10^{19}$ per g TiO_2. We may further suppose that the three peaks in the first stage correspond, respectively, to complexes having values of x of 1, 2, and 3, the last being the most easily reducible. Further discussion is not however justified at this stage. Reduction of these complexes gives very small Ir particles in the 1- to 2.5-nm range (Table 6).

We also believe that the Ir salt in excess of that required to form a monolayer exists as microcrystals of the salt after drying: these are less easily reduced than the adsorbed complexes ($T_{max} \geq 500$ K, Table 2), and afford larger (~10 nm) particles on reduction (Fig. 4). The manner in which the volumes of H_2 consumed in the two principal stages of TPR-I experiments (Fig. 6) varies with Ir content provides clear evidence for the formation of two different types of Ir particle.

The processes occurring during calcination as revealed by TPR-II, TPR-Ox, and HCl evolution experiments are less well understood. Calcination after a first reduction probably leads to Ir_2O_3 or to equivalent compounds of Ir^{III}: for example, residual Cl^- could form some oxo-chloro species of the kind described by Lieske *et al.* (*9*) in their studies of the Pt/Al_2O_3 system. The persistence of two peaks indicates that the small and large particles formed in TPR-I survive oxidation, but the differences in the volumes of H_2 consumed in the two stages suggests some structural changes. Prior calcination similarly may lead to oxo-chloro species; these are easily reducible ($T_{max} \sim 400$ K, Table 1), but the occurrence of a second peak again suggests that the structure formed during drying has remarkable persistence.

The ammine complex also exhibits two peaks in TPR (Fig. 3), indicating that it too may form a dispersed monolayer as well as microcrystals. However, T_{max} values are much higher than for the chloride salt, and for this reason the average particle size may be larger. Indeed, there is some support for this from electron microscopy, by which 3- to 5-nm particles were observed.

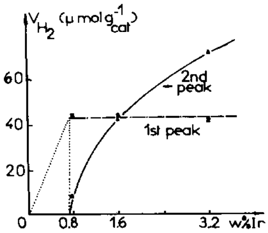

FIG. 6. Dependence of volume of H_2 consumed in the two principal sages of TPR-I experiments as a function of Ir content.

The least satisfactory aspect of the results and their interpretation is the values for H/Ir_{tot} found in reduction of the chlorocomplexes (Table 3). All are less than the theoretical value of three for Ir^{III}: we believe it is possible that there are reducing sites on the TiO_2 surface (*20*), and that some of the Ir^{III} is reduced to Ir^{I} before or during the drying stage. More work is needed to substantiate this idea.

We believe the presence of residual chloride on the catalysts has a marked effect on the O_2 titration results for TiO_2-supported catalysts (Table 6) and that it is responsible for the low estimates of the number of Ir_s atoms, and hence for the discrepancy between particle size estimates by this method and by electron microscopy. The way in which it may operate is as follows. To obtain a valid estimate of the number of Ir_s atoms, the water formed by reaction of O_2 with H_{ads} must vacate the Ir surface, freeing it for further O_2 chemisorption, and move to the support. If Ti—Cl groups are present near the Ir particles, migration of water to the support may be inhibited if Ti—OH groups are needed to hydrogen-bond the water as it moves. Alternatively residual Cl^- may partition itself between the support and the metal, acting as a poison when on the latter. Even HTR may leave sufficient residual Cl^- to interfere with O_2 titration at room temperature (Table 6). Substantially better agreement is found between particle size estimates by OT and by electron microscopy in the case of Ir/SiO_2 (Table 6).

This being so, the discrepancy between the TOF's for Ir/SiO_2 and LTR Ir/TiO_2 is qualitatively understandable; unfortunately we do not have an accurate particle size distribution obtained by electron microscopy, so quantitative comparison is not possible. The low TOF's found with HTR Ir/TiO_2 present a greater difficulty. One possible explanation is that the free sites remaining on particles of Ir in the SMSI state are crowded by adjacent TiO_{2-x} particles and are not freely accessible by the large benzene molecule. Thus only a fraction of the sites available for H_2 chemisorption may be effective for the hydrogenation; this may also serve to explain the very variable activation energy found with HTR catalysts.

It is reasonable to enquire whether the effect of residual Cl^- in TiO_2-supported catalysts has been observed before. Foger (*21*) has reported a very high dispersion for 1% Ir/TiO_2 by H_2 chemisorption, but the pretreatment he used (H_2, 773 K, 15 h; O_2, 673 K, 2 h; H_2, 473 K, 2 h) may have served to remove most of the Cl^- remaining from the H_2IrCl_6 salt which he used. In the seminal paper (*22*) Tauster and Fung actually found H/Ir = 1.17 after reduction at only 393 K; perhaps at this low temperature the residual Cl^- is unable to migrate back from support to metal and hence is not a poison. However, reduction at 523 K lowered the H/Ir ratio to 0.32; this we feel is as likely to be due to Cl^- poisoning as to incipient SMSI. Residual Cl^- has also recently been implicated in the difficulty found in obtaining sensible H/Ru ratios by H_2 chemisorption following reduction of $RuCl_3$/TiO_2 (*23*). This is not the occasion to attempt a comprehensive review of the possible interfering effects of Cl^- in SMSI studies: we do however feel that a complete reappraisal of the literature is in order.

Washing after LTR of catalyst I 3.2 (Cl) removes Cl^- and gives a slight increase in catalytic activity (Fig. 5c). In view of the uncertainty concerning the precise dispersions of the catalysts used (see above), we cannot be sure that Ir/TiO_2 free of Cl^- is significantly different in activity from Ir/SiO_2, but the difference if any is certainly small.

One further point deserves attention. The catalyst E 2(NH_3) made from the ammine complex loses much less of its activity on HTR than do those made from the chloride salt (Table 6). It is difficult to see how the absence of Cl^- might be responsible, and the effect is more probably due to this catalyst's somewhat larger particle size. Whatever the explanation, the importance of the choice of Ir salt in determining catalytic behaviour is underscored by this observation.

APPENDIX

Estimation of the "Monolayer Capacity" of the $IrCl_6^{3-}$ Ion on a TiO_2 Surface

1. Estimate based on the size of the $IrCl_6^{3-}$ ion. Taking the Ir—Cl bond length as 0.23 nm and the Cl van der Waals radius as 0.18 nm, the size d of the ion is

$$d = 2 \times 0.23 + 2 \times 0.18 = 0.82 \text{ nm}.$$

Assuming cubic packing of the ions, the average area occupied by each is $0.82^2 = 0.672$ nm^2. Taking the surface area of the TiO_2 as 50 m^2 g^{-1}, i.e., 5×10^{19} nm^2 g^{-1}, the number n of ions which can be accommodated is

$$n = 5 \times 10^{19}/0.672 = 7.44 \times 10^{19} \text{ ions g}^{-1}.$$

2. Estimate based on H_2 consumption in TPR-I. Assuming that only "monolayer" $IrCl_6^{-1}$ is reduced in the first stage, and that the process is Ir^{III} to Ir^0, the volume of H_2 consumed (about 43 μmol g^{-1} or 2.59×10^{19} molecules, Table 1) is sufficient to reduce $2.59 \times 10^{19}/1.5$ ions, i.e., the "monolayer capacity" is 1.73×10^{19} ions g^{-1}.

3. Estimate based on the number of $IrCl_6^{3-}$ ions in the 0.8 wt% Ir catalyst. We now calculate the number of $IrCl_6^{3-}$ ions in the catalyst containing 0.8 wt% Ir because according to the TPR-I result (Fig. 1) most of the H_2 is consumed in the first stage; no assumption is made concerning the stoichiometry of the reduction.

Ir (0.8 wt%), i.e., 0.8 g Ir per 100 g TiO_2, is equivalent to 4.16×10^{-5} mol Ir g^{-1} and hence to 2.5×10^{19} atoms Ir g^{-1} or to $IrCl_6^{3-}$ ions g^{-1}.

4. *Estimate based on the number of OH groups on the TiO_2 surface.* Taking the number of OH groups n_{OH} as 4.5 nm^{-2} (*18*), n_{OH} is 2.25×10^{20} g^{-1}. Now if the $IrCl_6^{3-}$ ion interacts with Ti—OH groups as

$$IrCl_6^{3-} + 6TiOH \rightarrow IrCl_3(OTi)_3 + 3HCl$$
$$\rightarrow IrCl_3(OTi)_3 + 3TiCl + 3H_2O$$

then n is $2.25 \times 10^{20}/6$, i.e., 3.7×10^{19} ions g^{-1}. If on the other hand the interaction is formulated as

$$IrCl_6^{3-} + 2TiOH \rightarrow IrCl_5(OTi) + TiCl + H_2O$$

the value of n becomes $2.25 \times 10^{20}/2$, i.e., 1.1×10^{20} ions g^{-1}.

5. *Conclusion.* The quantity of $IrCl_6^{3-}$ in the "monolayer" form ($1.7–2.5 \times 10^{19}$ ions g^{-1}, Estimates 2 and 3) is about half that estimated on the basis of each ion interacting with six Ti—OH groups (Estimate 4) and about a quarter of that corresponding to cubic packing of the ions (Estimate 1). The close correspondence of these values supports our conclusion that a large fraction of the Ti—OH groups interact with $IrCl_6^{3-}$ ions during the preparation of low-Ir-content catalysts.

ACKNOWLEDGMENTS

We are grateful for the assistance of Dr. M. R. Gelsthorpe in obtaining the TPR results on the supported ammine complex, and to a referee for drawing our attention to significant references concerning the reaction of HCl with titania surfaces.

REFERENCES

1. Marques da Cruz, G., Djega-Mariadassou, G., and Bugli, G., *Appl. Catal.* **17,** 205 (1985).

2. Basset, J. M., Dalmai-Imelik, G., Primet, M., and Mutin, R., *J. Catal.* **37,** 22 (1975).

3. Vannice, M. A., and Chou, P., *in* "Proceedings, 8th International Congress on Catalysis, Berlin, 1984," Vol. V, p. 99. Verlag Chemie, Weinheim, 1984.

4. Resasco, D. E., and Haller, G. L., *J. Catal.* **82,** 279 (1983).

5. Haller, G. L., Henrich, V. E., McMillan, M., Resasco, D. E., Sadeghi, H. R., and Sakellson, S., *in* "Proceedings, 8th International Congress on Catalysis, Berlin, 1984," Vol. V, p. 135. Verlag Chemie, Weinheim, 1984.

6. Meriaudeau, P., Ellestad, O. H., Dufaux, M., and Naccache, C., *J. Catal.* **75,** 243 (1982).

7. Fung, S. C., *J. Catal.* **76,** 225 (1982).

8. Bournonville, J. P., Frank, J. P., and Martino, G., "Preparation of Catalysts III," p. 81. Elsevier, Amsterdam, 1983.

9. Lieske, H., Lietz, G., Spindler, H., and Völter, J., *J. Catal.* **81,** 8 (1983).

10. Menon, P. G., and Froment, G. F., *J. Catal.* **59,** 139 (1979).

11. Mutin, R., thesis. Lyon, 1971.

12. Boudart, M., and Djega-Mariadassou, G., "La Cinétique des Réactions en Catalyse Hétérogene," Masson Ed., Paris, 1982: English translation, Princeton Univ. Press, 1984.

13. Marques da Cruz, G., Thèse de Docteur Ingenieur, Paris, 1983.

14. Blanchard, G., Charcosset, H., Guenin, M., and Tournayan, L., *Nouv. J. Chim.* **5,** 85 (1981).

15. Bureau-Tardy, M., communication Xème Colloque Franco-Polonais sur la Catalyse, Caen, 10–13 Sept. 1985.

16. Parfitt, G. D., Ramsbotham, J., and Rochester, C. H., *Trans. Faraday Soc.* **67,** 3100 (1971); Primet, M., Basset, J., Mathieu, M. V., and Prettre, M., *J. Phys. Chem.* **74,** 2868 (1970); Shastri, A. G., Datye, A. K., and Schwank, J., *Appl. Catal.* **14,** 119 (1985).

17. Bond, G. C., and Rajaram, R. R., unpublished work.

18. Bond, G. C., Fuller, M. J., and Molloy, L. R., *in* "Proceedings, 6th International Congress on Catalysis, London, 1976" (G. C. Bond, P. B. Wells, and F. C. Tompkins, Eds.), p. 356. The Chemical Society, London, 1976.

19. Herrmann, M., Kaluza, U., and Boehm, H. P., *Z. Anorg. Allg. Chem.* **372,** 308 (1970).

20. Che, M., Naccache, C., and Imelik, B., *J. Catal.* **24,** 328 (1972).

21. Foger, K., *J. Catal.* **78,** 406 (1982).

22. Tauster, S. J., and Fung, S. C., *J. Catal.* **55,** 29 (1978).

23. Bond, G. C., and Xu Yide, *J. Chem. Soc. Faraday Trans. 1* **80,** 3103 (1984).